Pulsatile discharging from polymeric scaffolds: a novel method for modulated drug release

Patricia T. Campana,[1] Alexandre Marletta,[2] Erick Piovesan,[2] Kelliton J. M. Francisco,[1] Francisco V. R. Neto,[2] Leandro Petrini Jr.,[1] Thiago R. Silva,[1] Danilo Machado,[2] Francesco Basoli,[3] Osvaldo N. Oliveira Jr.,[4] Silvia Licoccia,[5] and Enrico Traversa[6*]

[1]School of Arts, Sciences and Humanities, University of São Paulo (USP), Arlindo Bettio Av., 1000. São Paulo, 03828-000, Brazil

[2]Institute of Physics, Federal University of Uberlândia (UFU), João Naves de Ávila Av., 2121. Uberlândia 38408-100, Brazil

[3]Department of Engineering, University of Rome "Campus Bio-Medico di Roma", Alvaro del Portillo St., 21. Rome 00128, Italy

[4]Sao Carlos Institute of Physics, University of São Paulo (USP), CP 369, 13560-970, Sao Carlos, SP, Brazil

[5]Department of Chemical Science and Technologies, University of Rome "Tor Vergata". Via della Ricerca Scientifica St. Rome 00133, Italy

[6]School of Materials and Energy, University of Electronic Science and Technology of China, 610054, Xi'an, Shaanxi, China

*E-mail: traversa.enrico@gmail.com

Enrico Traversa
He joined the University of Rome Tor Vergata since 1988, where he is since 2000 a Professor of Materials Science and Technology, presently on leave. From 2017, he is The National 1000-Talent Distinguished Professor at the School of Energy and Materials of the University of Electronic Science and Technology of China (UESTC), Chengdu, China. He was PI at the WPI MANA at the National Institute for Materials Science (NIMS), Tsukuba, Japan (2009-2012), and Professor at the Xi'an Jiaotong University, China (2012-2017). Listed in the Essential Science Indicators/Web of Science as a highly-cited researcher, both in Materials Science and Chemistry categories, he is Fellow of the Electrochemical Society, of the European Ceramic Society, and of the European Academy of Sciences. His research interests include nanostructured materials for environment, energy, and healthcare.

Abstract

Controlled drug release holds the promise to revolutionize medicine, particularly if short-term and long-term releasing can be combined in a single system. We present here a new pulsatile release system, in which the pulses were achieved using 3D scaffolds of poly(L-lactic acid), PLLA. From a morphological characterization of the scaffold's surfaces, before and after releasing experiments at distinct pHs, we infer that release is governed by electrostatic interactions and the fractal geometry of the scaffolds. Furthermore, the scaffold can present a short-term (within hours) or long-term (several days long) releasing profiles by varying the pH, which opens the way for unprecedented drug release control.

Keywords: Poly(lactide), Fractal dimension, Scaffolds

1. Introduction

The harsh side effects of cytotoxic therapy, which is currently a widely used clinical method to treat patients with tumors, motivate address research in finding alternative treatment methods.[1] A promising approach is the emerging metronomic therapy, which consists of low and reiterated doses of cytotoxic drugs that are able to reprogramming tumor cells into differentiation and senescence.[2] This means that cancer cells are dismissed through the same turnover mechanism occurring in normal cells, thus being a promising strategy to treat patients with limited side effects.[3] Delivering drugs at stable, low concentrations in the body for sustained times is a major issue that can be addressed by embodying the drugs in protective delivery systems.[4]

Micelles[5], microspheres[6], micro[7,8] and nanoparticles[9,10] have been used as drug carriers and drug delivery systems, for both immediate and controlled release. Polymeric scaffolds have been designed for delivering small molecules such as growing factors[11,12], specific sequences of DNA[13,14], heparin[15], proteins[16], and small molecular weight drugs[17,18], all for tissue regeneration. Nanoporous poly(caprolactone) (PCL) membranes were capable of releasing bovine serum albumin (BSA) for over 120 days at a slow releasing rate with a zero-order kinetics due to the dominating diffusion mechanism.[19] In fact, structured membranes should be adequate for long-term releasing owing to their physically robust structures, since system damages are avoided during the course of drug release.[20] Therefore, polymeric 3D scaffolds that provide good support for cells seeding in tissue engineering are good candidates for extended release systems.

Scaffolds made with natural or synthetic polymers have been proposed for both tissue regeneration and drug delivery. The most used natural polymers include electrospun scaffolds of fibrin[21], chitosan[22] and collagen[23], chitosan nanocomposites[24], collagen matrix with hydroxyapatite microspheres[25], gelatin scaffolds with kondagogu gum[26], and alginate/hydroxyapatite gel scaffolds with gelatin microspheres[27]. As for synthetic polymers, isomers of the biodegradable polyester (poly(lactic acid)) are probably the most popular[28]. Due to their high melting point (up to 323K[5,29,30]), biocompatibility with body tissues, mechanical properties and easy processibility, poly(caprolactone) (PCL), poly(D, L-lactic-co-glycolic acid) (PLGA) and poly(L-lactic acid) (PLLA) are found in most drug delivery systems. PCL, whose flexible mechanical properties are essential for applications in dentistry[31], can be found as electrospun nanofibers with[32] or without[15,33-35] gelatin. Scaffolds fabricated with the gas-foaming technique are normally highly

porous, with pore size heterogeneously distributed.[36] PLGA scaffolds, also biocompatible and biodegradable, are produced as electrospun nanofibers[37,38], microspheres loaded onto collagen-based scaffolds[39], or alginate-containing scaffolds[11], fabricated via thermally-induced phase-separation (TIPS)[13], gas foaming[14] and gas-foaming/salt-leaching[17]. PLLA scaffolds are mainly found as nanofibers[37] and mixed with other polymers[38].

All of these scaffolds share a structural non-regularity: electrospun scaffolds have a random distribution of micro/nanofibers, while the other methods yield highly porous structures with no regularity. The releasing curves reported for such scaffolds are typical of continuous delivery [6,19,20,24,26,35-38], whose mechanism is fitted with mathematical models such as zero-order kinetics[19,20,32].

In this study, PLLA scaffolds prepared via directional thermally induced phase separation (dTIPS) were used as a model drug delivery system to release BSA. These scaffolds, developed by Mandoli et al[40], showed high porosity (97%) and porous interconnectivity (91%), with such porosity and perfusive architecture to exhibit a highly regular 3D arrangement. The results presented here qualify these scaffolds' structures as fractals, which seem to be responsible for a quantized release of the proteins. Since the releasing rates vary with pH, it is envisaged that the releasing pulses may be controlled by combining pH values and fractal geometry.

2. Experimental

Materials. PLLA polymer (Poly(L-lactide, Mw = 101,000 g/mol), sodium acetate, sodium borate, sodium phosphate, bovine serum albumin (BSA – 66.3kDa), PFO (Poly(9,9-di-n-hexylfluorenyl-2,7-diyl), 1,4-Dioxane, and fluorescein isothiocyanate, FITC (FluoroTag™ FITC Conjugation Kit) were purchased from Sigma-Aldrich (St. Louis, MO) and used without any further purification. All solutions were prepared using ultrapure Milli-Q water and all reagents were of analytical grade.

Protein labeling. Labeling of BSA with FITC was performed according to the technical bulletin from the manufacturer.[41] Briefly, protein and FITC were diluted in carbonate-bicarbonate buffer (0.1 m) and kept covered with aluminum, incubating for 2 h at room temperature with gentle stirring. The conjugated FITC was separated from its non-conjugated counterpart in a Sephadex G-25M column. The purified BSA-FITC was lyophilized for further use.

Fabrication of PLLA scaffolds. PLLA scaffolds with BSA-FITC or PFO were prepared by thermally-induced phase separation (TIPS) technique.[40,42] Briefly, the polymer solution was prepared by dissolving PLLA (150 mg) and BSA-FITC or PFO (15 mg and 1 mg) into 1,4-Dioxane (3.6 mL) under stirring for 2 h. The final solution was kept in a cooler at -40°C (233K) for 12 h. 1,4-Dioxane was removed by a water/ethanol (80%w/w) solution at 10°C (263K) for 2 or 3 days. The scaffolds were dried at room temperature. About 10% of the BSA-FITC initial mass was lost in this process.

Structural morphology of PLLA scaffolds. The morphology of PLLA scaffolds was studied with a field emission scanning electron microscope (FE-SEM, SUPRA™ 35, Carl Zeiss SMT, Oberkochen, Germany), after gold coating using a sputtering coater (EMITECH K550, 2.5 min, 25 mA). The secondary electron (SE) detector was used with the aim of focusing on the morphology and surface features. Main operating parameters included 10 keV as gun voltage and working distance of about 8 μm.

Surface topology was investigated with atomic force microscopy (AFM), using a Shimadzu scanning probe microscope (SPM-9600, Shimadzu Co. Tokyo, Japan) with a silicon cantilever in the tapping mode. Channel diameters for each scaffold were estimated from the FE-SEM photographs using WSXM software.[43] Channel ellipticity was estimated from the ratio of axes a/b > 1 or b/a > 1, for those that had two axes measured (see SI for additional details). The histograms were plotted with the Origin™ Software.

Fractal dimension calculations. Fractal dimensions were calculated also using WSXM software and FE-SEM images to calculate the perimeter (P) and surface area (S) of the hills. The plot of log(P) versus log(S), the linear fit and the angular coefficient calculations were performed with Origin™ Software. Further details can be found in the Supporting Information.

Protein release experiments. BSA protein release was followed by measuring the FITC fluorescence (from FITC-BSA) in solution, using a spectrofluorimeter (ISS PC1, Illinois, USA). Each sample, with the bottom cross section facing the solution, was immersed into sodium phosphate, sodium borate, sodium acetate buffer (PBA) solution (0.1 M), at pH 2, 5, 7.4 and 8. The final buffer composition (10 mL of each pH) was 0.1 M sodium phosphate + 0.1 M sodium borate + 0.1 M sodium acetate for each pH, with concentrated HCl addition in quantities that depended on the desired pH, as follows: for pH = 8.0, 343.3 μL; for pH = 7.4, 360.5 μL; for pH = 5.0, 454.9 μL, and for pH = 2, 540.7 μL. The samples immersed into each pH buffer were kept at 37°C (310K) in a closed rectangular quartz cuvette, as shown in Figure 1, during 45 days.

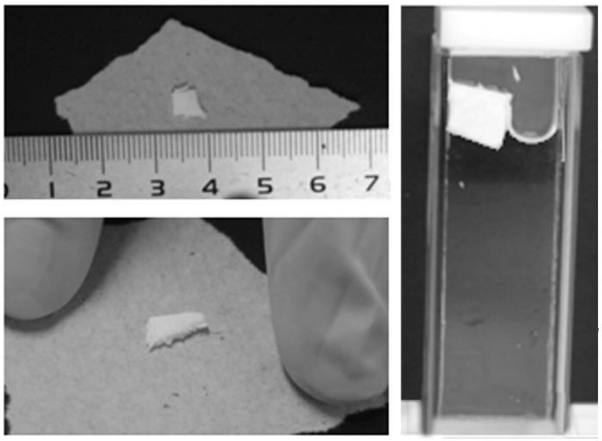

Figure 1. Size and experimental setup for protein delivery experiments.

Fluorescence measurements were done directly on the cuvettes. The excitation wavelength was 495 nm, and the emission spectra were recorded in the 305–700 nm range, with bandwidths of 2 nm for excitation and 1 nm for emission.

Poly(9,9-di-n-hexylfluorenyl-2,7-diyl) (PFO) release experiments. Poly(9,9-di-n-hexylfluorenyl-2,7-diyl), PFO, release experiments were performed by measuring PFO fluorescence in solution following the same process of the protein releasing experiments, but now using a laser from LASER Line model iZi operating at 457 nm as excitation source and an Ocean Optics 2000 spectrometer (Ocean Optics, Dunedin, USA) as light detector.

PFO anisotropy experiments. Anisotropy was probed using a laser from LASER Line model iZi operating at 457 nm as excitation source and an Ocean Optics 2000 spectrometer (Dunedin, USA) as light detector and a pair of polaroid to set the relation between the polarization of the excitation and the emitted light properly. When both excitation and emission have the same polarization direction, the signal is referred to as parallel. When excitation and emitted light are in perpendicular

polarization direction, the signal is referred to as perpendicular.

3. Results and Discussion

Releasing patterns. Release tests were made with PLLA 3D scaffolds prepared using the thermally-induced phase separation (TIPS) technique, according to Mandoli et al.[40,42] TIPS was developed in the 1980's[44,45] and consists in dissolving the polymer of interest in a high-boiling, low molecular weight solvent, forming a homogeneous solution, which is cooled to induce solute-solvent phase separation and polymer precipitation. The solvent is then extracted (often by freeze drying or by means of a leaching solution), resulting in a highly porous scaffold (or membrane) that can be varied by changing thermodynamic and kinetic parameters according to the temperature composition diagram for solvent and polymer.[46-48] Figure 2 shows the typical morphology of the PLLA 3D scaffolds; the SEM micrographs on the top ((a) and inset at higher magnification) and cross sectional (b) views show that the scaffolds featured regular internal channels (Fig. 2b), ending as pores at the surface (Fig. 2a).

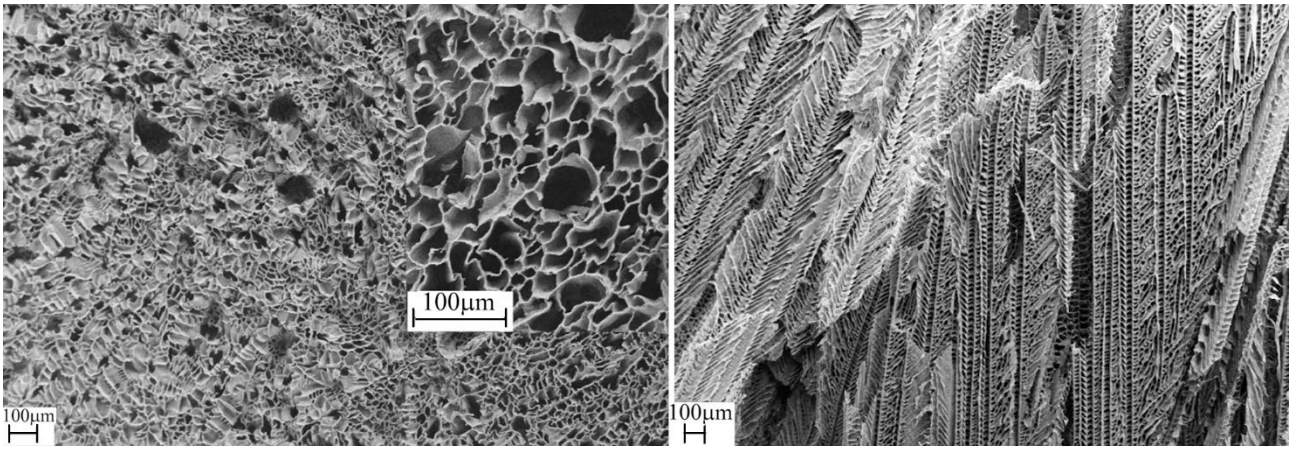

Figure 2. Typical SEM micrographs of the PLLA 3D scaffolds: top (a and inset at higher magnification) and cross sectional (b) views.

The majority of the vertically aligned channels are connected by lateral channels, forming knots at their connections points, thus resulting in a complex, porous structure.

Figure 3 shows the releasing profiles of FITC-BSA from the scaffolds upon immersion in acid (pH 2 and 5) and basic (pH 7.4 and 8) buffer solutions.

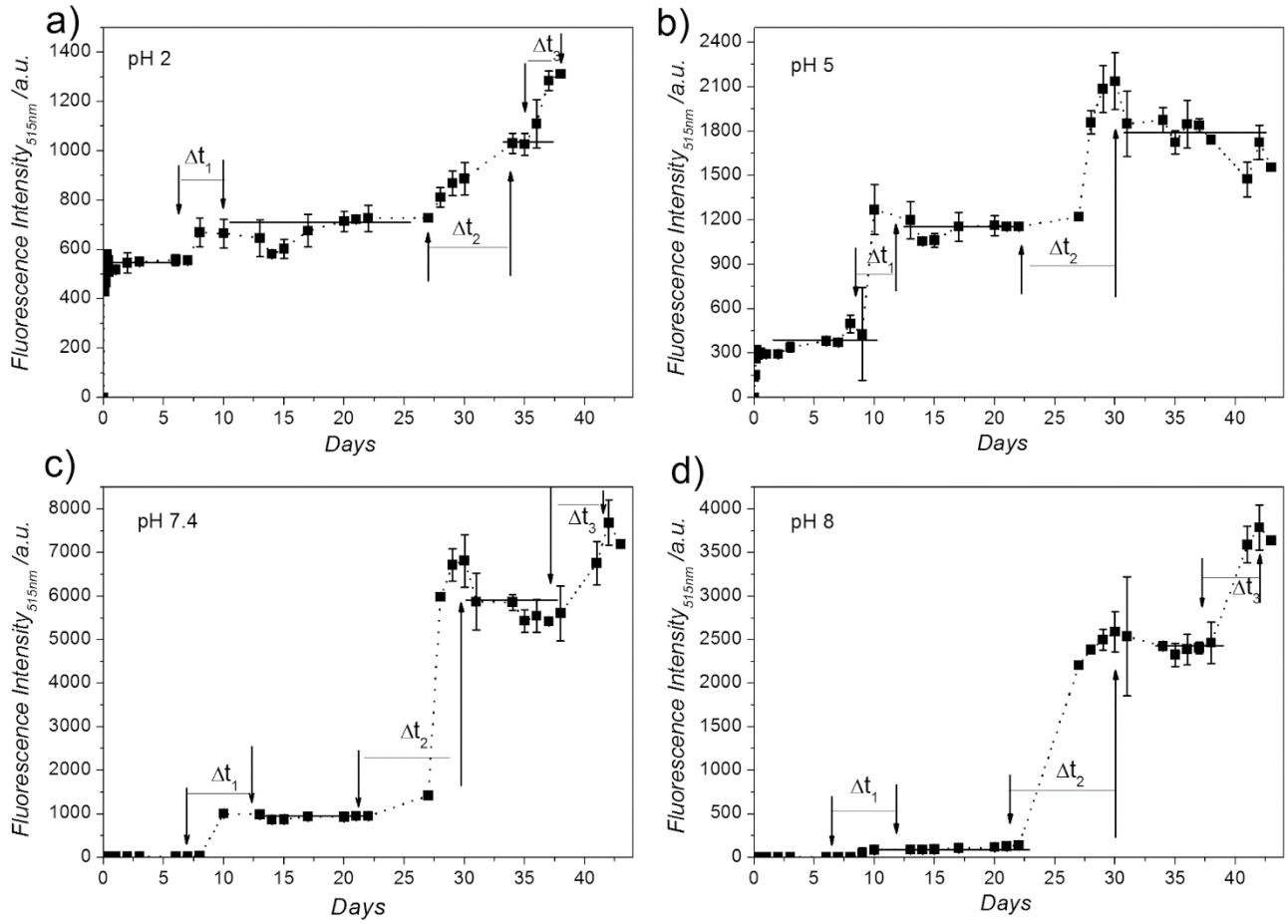

Figure 3. FITC-BSA fluorescence intensity at 515 nm during 45 days in acid (a, b) and basic (c, d) solutions. The arrows show values with zero derivative of the fluorescence intensity.

Although the intensities are not comparable, because the FITC fluorescence intensity increases with increasing pH[49], one readily sees that the protein release occurred in quantized steps. Therefore, the 3D PLLA scaffolds can be described as pulsatile release systems, with a given amount of proteins being released at different lapses of time.[50,51] With this stepwise behavior, the releasing curves cannot be fitted using the most common mathematical models, such as zero-order (which describes linear trends), Higuchi, or Korsmeyer-Peppas models[20,52] (see Supporting Information). Also, release starts faster in acidic pH, with the first release taking place some hours after immersion in solutions at pH 2 and 5 (Figure 3a and 3b), while for the basic pH values release occurred after more than five days (Figure 3c and 3d). Hence, other classifications should be used to identify the TIPS-PLLA scaffolds, in addition to be a pulsatile release. Following Singhvi and coworkers[20], this system could be classified as being typical of immediate release with release within the first hours at pH 2 and 5, and as delayed release at pH 7.4 and 8, in which the proteins' release occurs several days after immersion. Since the proteins keep being released for an extended period for all the pH values, the TIPS-PLLA scaffolds could also be classified as an extended release system. It is worth mentioning that even after 40 days of immersion some proteins remained in the scaffolds, as indicated by the yellowish color under an optical microscope. This observation confirms the extended release characteristic for this system, thus fulfilling one of the most important aspects of controlled release systems: to keep the drug concentration, in blood or in a specific tissue, for as long as possible.[22]

The difference in behavior for low and high pH values is attributed to the electrostatic interaction between the solvent and FITC-BSA, which are responsible for the release of the proteins from PLLA. At the acidic pH, especially at pH 2, in addition to the competition between the negative charges created by excess H^+, the acidic environment promotes partial protein unfolding, thus facilitating the protein release from the scaffold channels. At basic pH values, this effect disappears, and the immediate release did not occur. The releasing intervals (Δt) in Table 1 were estimated from the inflection points (zero derivative) in the releasing curves of Figure 3.Although the releasing process under acidic pH starts immediately and is delayed for basic pH, the intervals are very similar. In addition, the intervals appear to exhibit some regularity.

Table 1. Releasing intervals (Δt) in days at various pHs.

Δt	pH 2	pH 5	pH 7.4	pH 8
Δt_1	4	4	6	5
Δt_2	7	8	9	9
Δt_3	3	-	5	5

The interval increases ($\Delta t_2 > \Delta t_1$), and then decreases ($\Delta t_3 < \Delta t_2$) getting back to a value similar to the first one, which allows one to modulate the release.

For the sake of comparison, a different set of scaffolds was prepared containing Poly(9,9-di-n-hexylfluorenyl-2,7-diyl), PFO, instead of the labeled protein. The scaffolds were again immersed into the buffer solutions and no PFO fluorescence was observed after 45 days, at any of the pH values (2, 5, 7.4 and 8). Then, no detectable quantity of PFO was released from the scaffold structures. This signal absence could be due to a PFO/PLLA complex formation, in which PFO fluorescence would be quenched. This complex is not formed between FITC-BSA/PLLA, at least not in a way to quench FITC-BSA fluorescence, thus suggesting that the interactions between FITC-BSA/PLLA and PFO/PLLA are essentially different.

Fluorescence anisotropy was used to investigate whether the binding between PFO and PLLA had a favored direction, as "following" the channels together with PLLA. No anisotropy was detected in fluorescence measurements by exciting the cross section of the scaffolds (Bottom, Side and Up) (details in the Supporting Information). Therefore, the PFO/PLLA blend seems to have a homogeneous structure with isotropic distribution of PFO into the PLLA structure. As mentioned before, the lack of PFO fluorescence may be explained by a complex formation between PLLA and PFO; in other words, in terms of molecular interactions. The interaction between PFO and PLLA, which is basically hydrophobic, differs from the electrostatic interaction between the charged amino acids of FITC-BSA and the PLLA acidic terminations. The solvent electrostatic interactions with PFO and PLLA appear to be insufficient to overcome the energy barrier from the hydrophobic interactions.

Scaffold structure analysis and drug release properties. The most used models for drug delivery systems assume polymer degradation prior to the release[20], or that the polymer scaffold is porous, which would allow for release even if the scaffold structure is preserved. To test these hypotheses, we obtained AFM images with the samples before and after the releasing experiments. Figure 4 shows the surface topology for the scaffolds containing FITC-BSA, kept for 43 days in 100 mM phosphate/acetate/borate (PAB) buffer at pH 2. The root mean square roughness was σ_{RMS} = 0.058 μm, while for the scaffolds with no treatment σ_{RMS} = 0.024, suggesting that the treatment increased roughness[53].

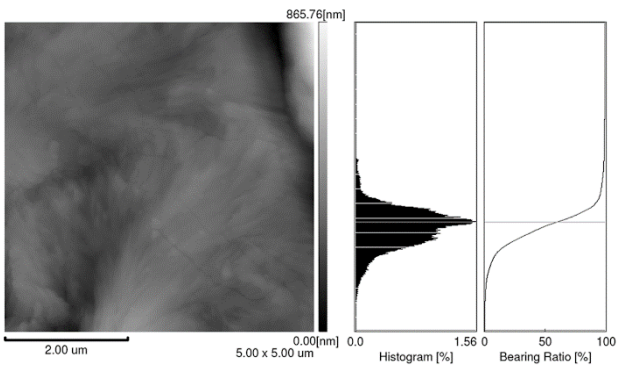

Figure 4. AFM height image of scaffold containing FITC-BSA after 43 days in PAB solution pH 2.

Similar results were obtained for scaffolds that remained 43 days into PAB pH 8, where σ_{RMS} = 0.095 μm, i.e., even larger. The value for Skewness (σ_{SK}) parameter, on the other hand, was negative (-1.649) for scaffolds at pH 8 and positive (1.434) for pH 2, which indicates a higher number of valleys at pH 8 and of hills at pH 2. The analyses of Kurtosis parameter (σ_{KU}) points to an increase in sharp peaks on the surface, since σ_{KU} decreases substantially from the scaffolds with no treatment (1965.18) for pH 2 (19.51) and pH 8 (9.59), indicating that all surface topologies are changed while the scaffolds were kept in solution

(Further details are given in the Supporting Information). The AFM images do not present significant changes on scaffolds' structures after 43 days; in other words, there was only a slight chemical abrasion in both pH 2 and 8. On the other hand, a homogeneous degradation could, in principle, lead to a minimal change in roughness. However, if this was the case, the degradation of scaffolds under distinct conditions would cause changes in morphology (and therefore roughness). Taken together, these results indicate that the proteins were released without considerable scaffold degradation since the film topography barely changed with the releasing experiments, even at extreme acidic and basic pH values.

Furthermore, optical images of the scaffolds after 40 days in PAB 100 mM pH 8 showed a considerable amount of BSA-FTIC (see Supporting Information), thus indicating that a large portion of the proteins were adsorbed on the channel walls. As these channels were hydrated with the acidic or basic solutions, protein release occurred owing mainly to the electrostatic interactions. However, electrostatic interactions and the slight degradation cannot alone account for the pulsatile release and the similarity between time intervals at different pH values (see Table 1). As will be discussed later, the geometry of the scaffolds seems to play an important role.

Channel size distribution measurements. The distribution of channel sizes in Figure 5 was obtained from six SEM images (three of them for each cross section: Bottom, Side and Up), totaling 8,449 channels (see Supporting Information). The distributions are not Gaussian for any of the cross sections.

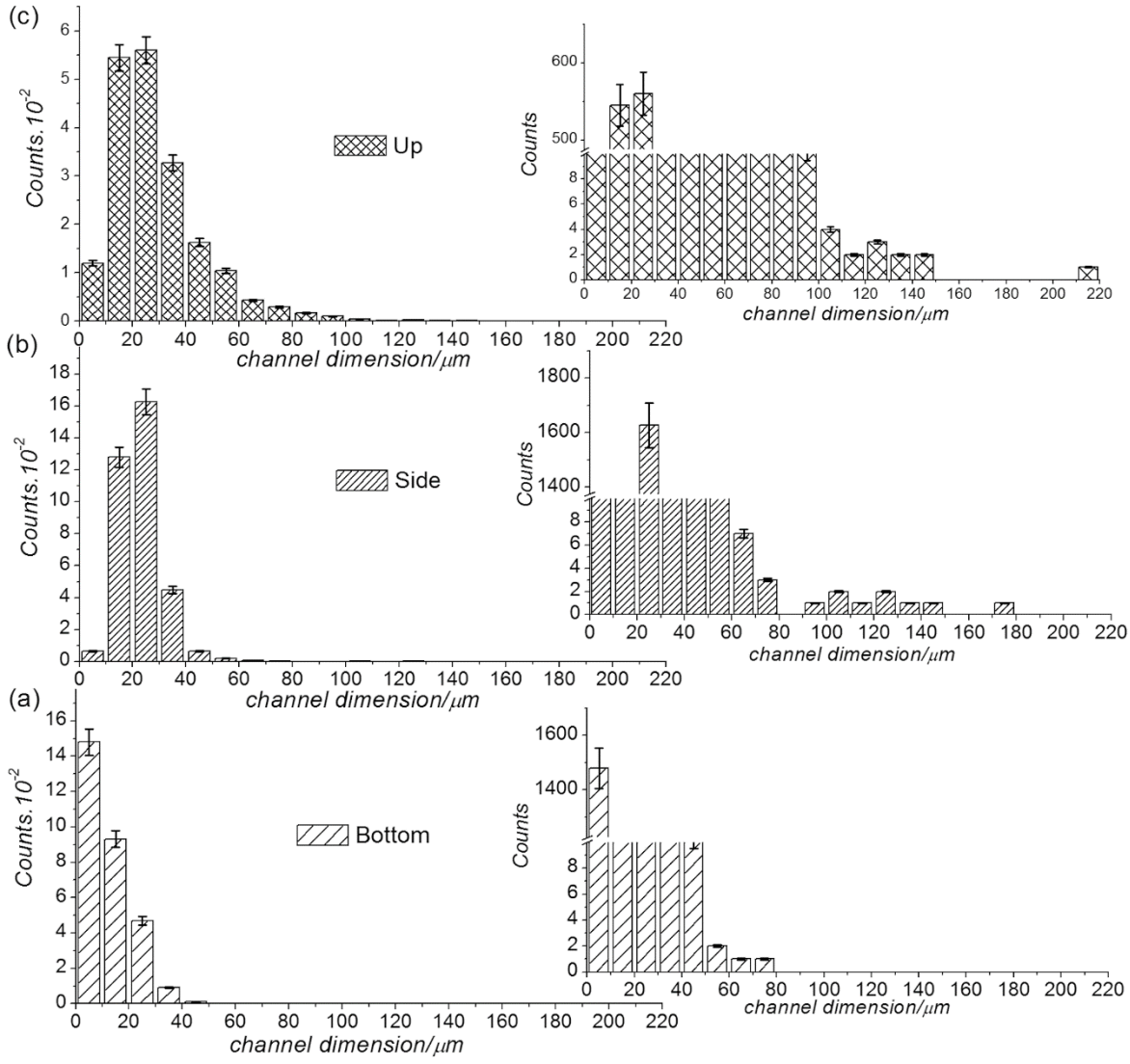

Figure 5. Channel size distribution for Bottom (a), Side (b) and Up (c) cross sections. The insets show the channels distribution focused on low occurrence values, in the interval between 0 and 220μm.

The channels appear smaller at the Bottom, at the sample/Teflon-container interface (Figure 5a), becoming larger alongside the sample (Side cross section, Figure 5b) until the top at the sample/air interface (Up cross section, Figure 5c). The distribution profile also indicates that channels growing from different directions come across each other to form knots with larger dimensions (up to 100 μm), which can be seen on the Side and Up cross sections (Figure 5b and 5c). To show the regularity of the channels, their ellipticity was estimated by the ratio of their axes, i.e. ellipticity is 1 for circular ones (further details in

the Supporting Information). Figure 6 shows an estimated ellipticity close to 1 for the majority of the channels for the three cross sections.

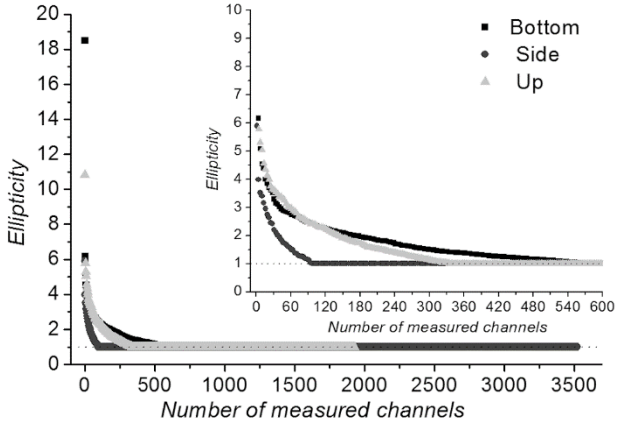

Figure 6. Estimated ellipticity for Bottom (squares), Side (circles) and Up (triangles) cross sections. The inset shows details at 0-600μm measured channels.

The inset in Figure 6 indicates that the Bottom cross section has a population of non-regular channels (ellipticity > 1), larger than for the Side and Up cross sections. This can be attributed to interface effects, since the Bottom cross section corresponds to the interface between the sample (FITC-BSA/PLLA) and sample holder. Because the latter is a Teflon container placed on a metallic surface in the cooler, heat exchange is certainly different between these materials, thus affecting the nucleation of 1,4-dioxane crystals[54,55], and consequently the polymer arrangement and the scaffold structure. At the Side cross section, this effect decreases strongly, about 5.5 times, probably due to a thermal equilibrium alongside the sample. Finally, at the Up cross section (interface sample/air), the interface effect is again observed, although less intense than that observed at the Bottom cross section.

Fractal Dimensions. The concepts of fractal geometry have been applied to natural and complex structures, e.g. macrophage membranes[56] and human malignant cells [57]. It can also be applied to specify 3-D topographies for irregular, rough or fragmented architectures[58]. This special geometry is characterized by the fractal dimension, D, obtained from the analyses of 2D surface structures. The D parameter can assume values between 2 (for a flat surface) and 3 (the highest fractal dimension)[26]. Table 2 reports the D values calculated for all the cross sections. D increases from the Bottom to Side cross sections (2.550 to 2.602) and then decreases from the Side to the Up cross sections (2.602 to 2.500) reaching a similar value to the initial one (Bottom cross section).

Table 2. Fractal Dimensions

	D'[a)]	Std[b)]	D[c)]	Std[d)]
Bottom	0.777	0.007	2.55	0.01
Side	0.801	0.007	2.602	0.007
Up	0.75	0.01	2.50	0.01

[a)]Slope for the linear plot of log(perimeter) versus log(area); [b)]Standard error; [c)]Fractal dimension; [d)]Standard error for fractal dimension.

From the results above, one notes an increase in fractal dimension at the scaffold interfaces (sample-holder/sample and sample/air). Because the materials at these interfaces are distinct, the thermal gradient during the TIPS process in these regions varies, resulting in structural differences. These changes in scaffold properties could be related to fractal dimension increments, as proposed by Smith and Mecholsky[59]. The observed variations in fractal dimensions have a coincident behavior with releasing time intervals (Δt_1, Δt_2, and Δt_3, Table 1). In other words, both time and fractal dimension variations are periodic, and, if one was able to extend the experiment for several months, it will be probably result in a sinusoidal curve for these two variations. These findings strongly suggest that both structural changes and increased fractal dimensions at interfaces (probably in a combined mechanism) are somehow related to the releasing time intervals. If, on the other hand, only degradation was driving the pulses, one should see the pulses being replaced by a continuous release as soon as the material started to degrade, resulting in a sigmoid curve instead of a periodic behavior. Furthermore, even at pH 7 where degradation is barely noticed, the pulses still exist. In subsidiary experiments we found that scaffolds with no variation in fractal dimensions release the drug in a continuous manner, which is consistent with the hypothesis of a pulsatile release depending on the fractal dimension.

4. Conclusion

In this work, we modified the fractal dimensions of PLLA 3D scaffolds which exhibited a pulsatile release for the PLLA/BSA-FICT system. The release rate could be varied by changing the pH, with immediate and faster release at acidic pH, or delayed and slower release at basic pH. Differently from other systems with pulsatile release, where structural properties are changed by combining systems with different structures[60-64], the PLLA 3D scaffolds were intrinsically modified by promoting changes in fractal geometry. Together with electrostatic interactions between the protein and the scaffold, the fractal geometry was responsible for the pulsatile release. Even though the release profile also depends on pH, pulsatile profiles were observed for a wide pH range. Therefore, a pulsatile release is likely for proteins other than BSA as long as there are scaffolds with fractal dimensions. Because fractal dimensions can be related to porosity and architecture of polymeric scaffolds,[66,67] if one can control the scaffold structure by varying the polymer/solvent equilibrium and thermodynamic parameters in the TIPS process, it would be possible to control the pulses and perhaps the releasing intervals (Δt). Significantly, varying pH and fractal geometry of the scaffolds can lead to both effective therapeutic concentration and adequate releasing times, suitable for different drug structures, administration routes, and therapies.

Acknowledgements

P.T.C. and A.M. contributed equally to this work. The authors would like to thank Ms. Heidi C. Piva for Graphical Abstract design. This work was supported by the Brazilian agencies CNPq [grant 474957/2013-6] and FAPESP [grants 2010/06728-8; 2012/13596-6 and 2013/14262-7].

Supporting Information

Releasing patterns fitted by Higuchi and Korsmeyer-Peppas models; PFO's fluorescence anisotropy; quantitative topology analysis of scaffolds' AFM images; optical image of the scaffold after 40 days in PAB 100mM pH 8; channel size and distribution measurements, Fractal Dimension

calculations. This material is available on http://dx.doi.org/10.1246/bcsj.***

References

1. H.R. Mellor, R. Callaghan, *Pharmacology* **2008**,*81*, 275.
2. A. K. Larsen, *Ann. Oncol* **1994**,*5*, 679.
3. C. Hart, M. Vogelhuber, D. Wolff, S. Klobuch, L. Ghibelli, J. Foell, S. Corbacioglu, K. Rehe, G. Haegeman, S. Thomas, W. Herr, A. Reichle, *Cancer Microenviron.* **2015**, *8*,75.
4. M. De Nicola, E. Bruni, E. Traversa, L. Ghibelli, *Nanomedicine: Nanotechnol. Biol. Medicine* **2017**, *13*, 2005.
5. T. K. Dash, V. B. Konkimalla, *J. Controlled Release* **2012**, *158*,15.
6. S. Li, S. Cai, B. Liu, K. Ma, Z. Wang, X. Li, *Acta Pharmacol. Sin.* **2006**, *27(6)*, 754.
7. K. G. Carrasquillo, A. M. Stanley, J. C. Aponte-Carro, P. De Jésus, H. R. Costantino, C. J. Bosques, K. Griebenow, *J. Controlled Release* **2001**, *76(3)*, 199.
8. B. Bittner, B. Ronneberger, R. Zange, C. Volland, J. M. Anderson, T. J. Kissel, *J. Microencapsul.***1998**, *15*, 495.
9. M. De, P. S. Ghosh, V. M. Rotello, *Adv. Mater.* **2008**, *20*, 4225.
10. M. E. Davis, Z. G. Chen, D. M. Shin, *Nat. Rev. Drug Discov.* **2008**, *7(9)*, 771.
11. A. Perets, Y. Baruch, F. Weisbush, G. Shoshany, G. Neyfeld, S. Cohen, *Mater. Res.* **2003**, *65(4)*, 489.
12. W. L. Murphy, M. C. Peters, D. H. Kohn, D. J. Mooney, *Biomaterials* **2000**, *21(24)*, 2521.
13. K.W. Chun, K. C. Chow, S. H. Kim, J. H. Jeong, T. G. Park, *J. Biomater. Sci.* **2004**, *15*, 1341.
14. J. Jang, C. B. Rives, L. D. Shea, *Molec. Ther.* **2005**, *12(3)*, 475.
15. E. Luong-Van, L. Grøndahl, K. N. Chua, K. W. Leong, V. Nurcombe, S. M. Cool, *Biomaterials* **2006**, *27(9)*, 2042.
16. A. Szentivanyi, U. Assmann, R. Schuster, B. Glasmacher, Materialwiss. Werkstofftech. **2009**, *40*, 65.
17. J. J. Yoon, J. H. Kim, T. G. Park, *Biomaterials* **2003**, *24(13)*, 2323.
18. J. Chen, C. Wang, S. Lü, J. Wu, X. Guo, C. Duan, L. Dong, Y. Song, J. Zhang, D. Jing, L. Wu, J. Ding, D. Li, *Cell Tissue Res* .**2005**, *319(3)*, 429.
19. D. A. Bernards, K. D. Lance, N. A. Ciaccio, T. A. Desai, *Nano Lett* **2012**., *12(10)*, 5355.
20. D. Fine, A. Grattoni, S. Hosali, A. Ziemys, E. De Rosa, J. Gill, R. Medema, L. Hudson, M. Kojic, M. Milosevic, L. Brousseau III, R. Goodall, M. Ferrari, X. Liu, *Lab Chip* **2010**, *10(22)*, 3074.
21. C. Dwivedi, H. Pandey, A. C. Pandey, P. W. Ramteke, *Curr. Pharm. Des.* **2016**, *22(11)*, 1460.
22. X. Zhaoa, S. Chena, Z. Lina, C. Dua, *Carbohydr. Polym.* **2016**, *148*, 98.
23. G. Rath, T. Hussain, G. Chauhan, T. Garg, A. K. Goyal, *J. Drug Targeting* **2016**, *24(6)*, 520.
24. A. B. Reddy, B. Manjula, T. Jayaramudu, E. R. Sadiku, P. A. Babu, S. P. Selvam, *Nano-Micro Lett.* **2016**, *8(3)*, 260.
25. R. Cholas, S. K. Padmanabhan, F. Gervaso, G. Udayan, G. Monaco, A. Sannino, A. Licciulli, *Mater. Sci. Eng. C* **2016**, *63*, 499.
26. H. S. Rathore, M. Sarubala, G. Ramanathan, S. Singaravelu, M.D. Raja, S. Gupta, U. T. Sivagnanam, *Mater. Lett.* **2016**, *177*, 108.
27. J. Yan, Y. Miao, H. Tan, T. Zhou , Z. Ling, Y. Chen, X. Xing, X. Hu, Mater. *Sci. Eng.C* **2016**, *63*, 274.
28. H. Seyednejad, A. H. Ghassemi, C. F. van Nostrum, T. Vermonden, W. E. Hennink, *J. Controlled Release* **2011**, *152(1)*, 168.
29. Guoguang Xu, Xiao Liu, Yanqun Lin, Guoshan He, Wanjuan Wang, Wen Xiong, Haiying Luo, Zhong Liu, Jianhao Zhao, *J. Appl. Polym. Sci.* **2015**, *132*, 42064.
30. N. Faisant, J. Siepmann, J.P. Benoit, *Eur. J. Pharm. Sci* .**2002**, *15(4)*, 355.
31. M. A. Woodruff, D. W. Hutmacher, *Prog. Polym. Sci.* **2010**, *35(10)*,1217.
32. X. Zhu, S. Ni, T. Xia, Q. Yao, H. Li, B. Wang, J. Wang, X. Li, W. Su, *J. Pharm. Sci.* **2015**, *104(12)*, 4345.
33. S. Soliman, S. Pagliari, A. Rinaldi, G. Forte, R. Fiaccavento, F. Pagliari, O. Franzese, M. Minieri, P. Di Nardo, S. Licoccia, E. Traversa, *Acta Biomater.* **2010**, *6(4)*, 1227.
34. S. Soliman, S. Sant, J. W. Nichol, M. Khabiry, E. Traversa, A. Khademhosseini, *J. Biomed. Mater. Res. A* **2011**, *96(3)*, 566.
35. M. Ranjbar-Mohammadi, S. H. Bahrami, *Int. J. Biol. Macromol.* **2016**, *84*, 448.
36. A. Salerno, J. Saurin, C. Domingo, *Int. J. Pharm*. **2015**, *496*, 654.
37. W. Liu, J. Wei, Y. Chen, *New J. Chem.* **2014**, *38*, 6223.
38. W. Zhu, S. Liu, J. Zhao, S. Liu, S. Jiang, B. Li, H. Yang, C. Fan, W. Cui, *Acta Biomater.* **2014**, *10*, 3018.
39. S. Minardi, B. Corradetti, F. Taraballi, M. Sandri, J. O. Martinez, S. T. Powell, A. Tampieri, B. K. Weiner, E. Tasciotti, *Small* **2016**, *12(11)*,1479.
40. C. Mandoli, B. Mecheri, G. Forte, F. Pagliari, S. Pagliari, F. Carotenuto, R. Fiaccavento, A. Rinaldi, P. Di Nardo, S. Licoccia, E. Traversa, *Macromol.Biosci.* **2010**, *10(2)*, 127.
41. FluoroTag™ FITC Conjugation Kit Technical Bulletin, http://www.sigmaaldrich.com/content/dam/sigma-aldrich/docs/Sigma/Bulletin/fitc1bul.pdf, accessed: June, **2016**.
42. C. Mandoli, E. Traversa E, (Dokuritsu Gyosei Hojin Busshitsu Zairyo, NIMS-C), US2011171732-A1, JP2011160797-A, **2011**.
43. I. Horcas, R. Fernández, J. M. Gómez-Rodríguez, J. Colchero, J. Gómez-Herrero, A. M. Baro, *Rev. Sci. Instrum. , 78(1-013705)*, 1.
44. G. T. Caneba, G. S. Soong, *Macromolecules* **1985**, *18(12)*, 2538.
45. G. T. Caneba, G. S. Soong, *Macromolecules* **1985**, *18(12)*, 2545.
46. H. J. Chung, T. G. Park, *Adv. Drug Delivery Rev* .**2007**, *59(4-5)*, 249.
47. J. F. Kim, J. H. Kim, Y. M. Lee, E. Drioli, *AIChE J.* **2016**, *62*, 461.
48. D. R. Lloyd, S. S. Kim, K. E. Kinzer, *J. Memb. Sci***1 991**, *64(1-2)*, 1.
49. A. Schulz, S. Hornig, T. Liebert, E. Birckner, T. Heinzeb, G. J. Mohr, *Org. Biomol. Chem.***2009**, *7*, 1884.
50. G. Singhvi, M. Singh, *Int. J. Pharm. Studies and Res.* **2011**, *II(I)*, 77.
51. C. K. Sahoo, S. R. M. Rao, M. Sudhakar, K. Stayanarayana, *Der Pharm. Lett.* **2015**, *7(9)*, 186.
52. S. Dash, P. N. Murthy, L. Nath, P. Chowdhury, *Acta Pol. Pharm.* **2010**, *67(3)*, 217.
53. E. M. Therézio, M. L. Vega, R. M. Faria, A. Marletta, InTechOpen (CC BY 3.0 license), **2012**, Ch.3.
54. C. J. Jacobs, G. S. Parks, *J. Am. Chem. Soc.* **1934**, *56(7)*, 1513.
55. S.-J. Kim, J.-Y. Nam, Y.-M. Lee, S.-S. Im, *Polymer* **1999**, *40*, 5623.
56. A. Bitler, R. Dover, Y. Shai, *Micron.* **2012**, *43(12)*, 1239.
57. M. E. Dokukin, N. V. Guz, C. D. Woodworth, I. Sokolov,

New J. Phys. **2015**, *17(3,033019)*, 1.
58. B.B. Mandelbrot, D. E. Passoja, A. J. Paullay, *Nature* **1984**, *308*, 721.
59. R. L. Smith, J. J. Mecholsky Jr., *Mater. Charact.* **2011**, *62(5)*, 457.
60. N. Jain, V. K. Devi, *Ind. Crops Prod.* **2016**, *88*, 58.
61. X. Liu, G. J. Pettway, L. K. McCauley, P. X. Ma, *Biomaterials* **2007**, *28(28)*, 4124.
62. T. Barroso, R. Viveiros, T. Casimiro, A. Aguiar-Ricardo, *J. Supercrit. Fluids* **2014**, *94*,102.
63. A.W. Chan, R.A. Whitney, R.J. Neufeld, *Biomacromolecules* **2009**, *10(3)*, 609.
64. S. Y. Tzeng, R. Guarecuco, K. J. McHugh, S. Rose, E. M. Rosenberg, Y. Zeng, R. Langer, A. Jaklenec, *J. Control. Release* **2016**, *10(233)*, 101.
65. Q. Shi, Y. Zhou, Y. Sun, *Biotechnol. Prog.* **2005**, *21(2)*, 516.
66. F. A. Macedo, E. H. M. Nunes, W. L. Vasconcelos, R. A. Santos, R. D. Sinisterra, M. E. Cortes, *Cêramica* **2012**, *58*, 481.
67. S. Sánchez-Salcedo, F. Balas, I. Izquierdo-Barba, M.Vallet-Regí, *Acta Biomater*. **2009**, *5(7)*, 2738.

Graphical Abstract

Pulsatile discharging from polymeric scaffolds: a novel method for modulated drug release

Patricia T. Campana, Alexandre Marletta, Erick Piovesan, Kelliton J. M. Francisco, Francisco V.R. Neto, Leandro Petrini Jr., Thiago R. Silva, Danilo Machado, Francesco Basoli, Osvaldo N. Oliveira Jr., Silvia Licoccia, and Enrico Traversa.

We introduce a new pulsatile release system, using PLLA 3D scaffolds and performing releasing experiments at distinct pH. We infer that release is governed by electrostatic interactions and the scaffolds' fractal geometry. Furthermore, the scaffold can present a short-term (within hours) or long-term (several days long) releasing profiles by varying the pH, which opens the way for unprecedented drug release control.